Mesospheric density measured by Rayleigh lidar over Golmud

Qiao Shuai[1,2], Pan Weilin[1,2], Ban Chao[1], Zhang Hengheng[1,3]

(1. Key Laboratory of Middle Atmosphere and Global Environment Observation, Institute of Atmospheric Physics, Chinese Academy of Sciences, Beijing 100029, China;
2. University of Chinese Academy of Sciences, Beijing 100049, China;
3. School of Atmospheric Physics, Nanjing University of Information Science and Technology, Nanjing 210044, China)

Abstract: The MARMOT (Middle Atmosphere Remote Mobile Observatory in Tibet) lidar had been deployed at Golmud (36.25 °N, 94.54 °E), Qinghai Province, for measuring the mesospheric density from 50 to 90 km from August 2013 to October 2015. An improved method for Rayleigh lidar retrieval of the mesospheric density was proposed, by using the TIMED/SABER satellite data at 50 km as the reference value. The results show that the lidar derived densities are consistent with the satellite data. However, both the lidar and satellite measurements of mesospheric densities are mostly lower than the MSIS-00 model, with the largest discrepancies occurred at 75-90 km in winter.

Key words: Rayleigh lidar; atmospheric density; MSIS model; TIMED/SABER satellite
CLC number: P413 **Document code:** A **DOI:** 10.3788/IRLA201847.S106005

基于瑞利激光雷达对格尔木中间层大气密度的探测研究

乔 帅[1,2],潘蔚琳[1,2],班 超[1],张衡衡[1,3]

(1. 中国科学院大气物理研究所 中层大气与全球环境探测重点实验室,北京 100029;
2. 中国科学院大学,北京 100049; 3. 南京信息工程大学 大气物理学院,江苏 南京 210044)

摘 要: 2013 年 8 月到 2015 年 10 月,利用 MARMOT 激光雷达对青海格尔木(36.25 °N,94.54 °E) 上空 50~90 km 高度的中间层大气密度进行了探测。利用 TIMED/SABER 卫星在 50 km 高度探测的大气密度作为参考数据,提出了一种瑞利激光雷达探测大气密度的改进算法。结果表明,在中间层高度范围内,激光雷达的大气密度探测结果与 TIMED/SABER 卫星数据的一致性较好,二者的结果基本均低于 MSIS-00 模式值,尤其在冬季 75~90 km 高度存在较大偏差。

关键词: 瑞利激光雷达; 大气密度; MSIS 模式; TIMED/SABER 卫星

收稿日期: 2018-03-05; **修订日期:** 2018-05-13
基金项目: 国家自然科学基金(41127901)

作者简介: 乔帅(1988-),男,博士生,主要从事激光雷达大气遥感方面的研究。Email:qiaoshuai@mail.iap.ac.cn
导师简介: 潘蔚琳(1973-),女,研究员,博士生导师,博士,主要从事中高层大气主、被动光学遥感探测系统方面的研究。
Email:panweilin@mail.iap.ac.cn

0 Introduction

The dynamics and chemistry of middle atmosphere is believed to have a close relationship with the global climate change[1-2]. Middle atmosphere interacts with both the troposphere and the thermosphere through dynamical processes, such as tides, planetary waves, and gravity waves[2-4]. For better understanding of the middle atmosphere, it is necessary to obtain atmospheric parameters such as atmospheric density[5]. Accurate measurements and predictions of the neutral density in the middle atmosphere are also critical for low-Earth-orbit satellite operations, including orbit determination and re-entry calculation.

Thermospheric density is usually inferred from accelerometer measurements on satellites[6]. Neutral density below 30 km can be obtained from radiosonde. However, mesospheric density has not yet been measured extensively, because of limited probing technology for decades. Rockets were occasionally launched for making in-situ measurement of neutral density up to the mesosphere[7-9]. Since the 1980s, lidar technique has been proven an effective tool for profiling atmospheric density in the middle atmosphere[10-13]. Hauchcorne and Chanin described the principle of Rayleigh lidar and reported the first lidar measurements of middle atmosphere density and temperature[10]. Shibata et al. used a XeF lidar for neutral density measurements[11]. Deng et al. measured the density and temperature in the middle atmosphere with a Rayleigh lidar at Hefei, China[13].

From August 2013 to October 2015, MARMOT (Middle Atmosphere Remote Mobile Observatory in Tibet) lidar was operated at Golmud, Qinghai (36.25 °N, 94.54 °E; 2800 MSL). In this paper, we describe an improved method to derive mesospheric density using Rayleigh lidar technique. The lidar results were then compared with the satellite measurements and model data.

1 Instrument and database

1.1 MARMOT lidar

The MARMOT lidar consisted of a laser transmitter, an optical receiver, and a signal acquisition & control unit [14-15]. The main part of the laser transmitter was a Nd:YAG laser working at 532 nm wavelength. The optical receiver was a prime focus telescope of Φ1 000 mm, collecting the backscattered signals from the altitude of 50-90 km. A mechanical chopper was used in the receiver for blocking lidar signals below 50 km, in order to avoid PMT saturation caused by strong signal returns from low altitudes.

From 2013 to 2015, MARMOT lidar has made a total of 205 nights of observation at Golmud, located in the northeast part of Tibetan Plateau. The minimal observational span per night is about 2 hours, while typical observation length per night is about 8 hours. We made a composite dataset with three years of lidar data, and used the daily averaged density profiles for data analysis. The total observation days of each season are listed in Tab.1.

Tab.1 Observation days of MARMOT lidar for four seasons at Golmud

Season	Months	Days
Spring	March-May	22
Summer	June-August	55
Autumn	September-November	89
Winter	December-February	39

1.2 TIMED/ SABER satellite

SABER (The Sounding of the Atmosphere using Broadband Emission Radiometry) is a multichannel radiometer onboard the TIMED (Thermosphere Ionosphere Mesosphere Energetics and Dynamics) satellite, launched in 2001. TIMED/SABER can provide global coverage of the atmospheric density from 15 km up to 120 km[16]. However, satellite cannot make continuous measurements over one single site at

high time resolution. On the other hand, lidar can provide high temporal and spatial resolution measurements for investigating the variations caused by atmosphere waves.

In this paper, we chose all the density profiles measured by this satellite during the lidar observation night over an area within ±5° latitude and ±10° longitude from the location of Golmud. Typically about 2–4 satellite density profiles were averaged for each night.

1.3 NRLMSIS-00 model

NRLMSIS (Mass Spectrometer and Incoherent Scatter empirical model, hereinafter referred to as MSIS-00) is an empirical global scale model of the Earth′s atmosphere[17]. It can provide vertical distributions of atmosphere parameters, such as neutral density, from ground up to the space. In this paper, we used the MSIS-00 model data during the same period of lidar operation in Golmud.

2 Method

Rayleigh lidar backscattered signal is proportional to the atmospheric density. After compensating the range dependency factor, we can obtain relative density profiles. If the absolute density value at a reference altitude is given, the density profiles can be obtained in Eq.(1).

$$\rho(z)=\frac{z^2\rho(z_0)(N(z)-N_B)}{z_0^2(N(z_0)-N_B)} \tag{1}$$

where $\rho(z)$ is atmospheric density at the altitude z; $N(z)$ is lidar received signal at the altitude z; N_B is background noise; $\rho(z_0)$ is the density at the reference altitude z_0. Due to the fact that atmospheric density decreases exponentially with the altitude, we used 50 km as z_0, where signal-to-noise-ratio(SNR) highest for the entire 50–90 km altitude range. The Rayleigh scattered signals above 110 km are negligibly weak, therefore in our study, photon counts at 115–125 km altitude were averaged for estimating the background level.

A typical nightly mean relative density profile was derived using the MARMOT lidar observation and shown in Fig.1(a), with the corresponding relative uncertainty shown in Fig.1 (b). The neutral density decreased exponentially from 50 to 90 km, while densities at 90 km were nearly three orders of magnitude lower than those at 50 km.

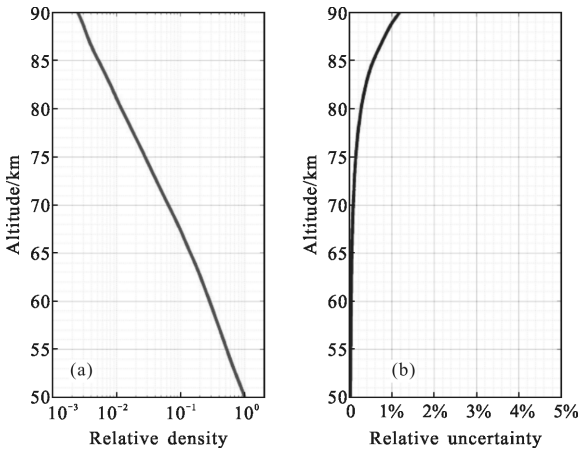

Fig.1 Relative density profile (a) and uncertainties (b) derived from MARMOT lidar data on December 27th, 2014

Measurement uncertainties were mainly caused by the fluctuations of the received photon counts, which satisfy the Poisson distribution, so its standard deviation equals to square root of mean value, as in Eq.(2):

$$\sigma_N=\sqrt{N} \tag{2}$$

In our case, N_B is relatively low for nighttime lidar observations, therefore the relative uncertainty of density can be expressed as Eq.(3):

$$\frac{\Delta\rho}{\rho}\approx\frac{\sqrt{N}}{N-N_B} \tag{3}$$

In order to achieve a sufficient SNR, especially at higher altitudes where molecular density is extremely low, the density profile was calculated by adding up a total of 5.5 hours of lidar data throughout the whole night on December 27th, 2014. Vertical resolution was reduced to 300 m by signal binning.

Traditional method normally calculated atmospheric density by multiplying the lidar derived relative density profile with a reference density value chosen from a model (for example, MSIS-00) at a

certain altitude[13]. However, in the mesosphere region, there exist certain deviations between the model and the observed densities[18]. Consequently, the density profile obtained using this method could deviate from the actual values. Here we propose an improved method for density calculation by using the satellite measured density at 50 km as the reference. In the next section, lidar results using this improved method are presented and then compared with the traditional method using model data as the reference.

3 Results

Nightly mean density profiles were averaged to yield the mean density profiles for each of the four seasons. To better illustrate the density differences among the lidar, satellite, and model, we define the density ratio as the ratio of density measurement to the MSIS-00 model density. In Fig.2, density ratio profiles were plotted for spring, summer, autumn and winter, respectively. In each panel, black solid line is the lidar density ratio using our new method (by adopting satellite density at 50 km as the reference), grey solid line is the lidar density ratio using traditional method (by adopting model density at 50 km as the reference), the black dashed line is the satellite density ratio, while model density ratio is plotted as grey dashed line with a constant of 1.

From the figure, we can see that there is merely an offset between the black solid line and the grey solid line, because different values of density at reference altitude were applied. On the other hand, it is clear to see that the lidar results (shown in black solid line) using our proposed new method were much closer to satellite results(in black dashed line) than the results from traditional method(shown in grey solid line).

In spring, lidar density agreed very well with satellite density between 50-70 km, while both observations about 1%-6% lower than the model. Between 70-76 km, lidar, satellite, and model data were in good agreement. Lidar density was slightly (about 1%-3%) higher than satellite data between 77-90 km.

In summer, lidar density and satellite density were consistent with each other between 50-82 km, while both observations about 5%-11% lower than the model. Between 82-90 km, lidar density was slightly (about 1%-5%) higher than satellite data, which was about 10% lower than the model.

In autumn, lidar density agreed very well with satellite density between 50-77 km, while both observations about 5%-8% lower than the model. Between 77-90 km, lidar density was slightly (about 1%-3%) higher than satellite data, while both observations about 8%-17% lower than the model.

In winter, lidar density agreed very well with satellite density between 50-73 km, while both observations about 3%-13% lower than the model. Between 73-90 km, lidar density was slightly different from satellite data by about 2%, while both observations about 13%-19% lower than the model. Notably, the differences between observations (lidar or satellite) and model were largest in winter among four seasons between 75-90 km.

Overall, if the satellite data at 50 km were used as the reference for lidar density derivation, the results (in black solid lines) were constant with the satellite data (in black dashed lines) between 50-75 km. Nevertheless, they exhibited certain deviations from each other between 75-90 km. This could be explained by the fact that lidar measurement uncertainties increase with the altitude, as shown in Fig.1(b).

To further evaluate our improved method, we calculated the standard deviations (std) between the lidar density ratios and the satellite density ratio and listed them in Tab.2. It showed that the mesospheric densities using the newly improved lidar method are much more consistent with satellite results, compared with the traditional lidar method. It also indicates that the atmospheric densities simulated by MSIS-00 model are not always accurate in the mesosphere

region.

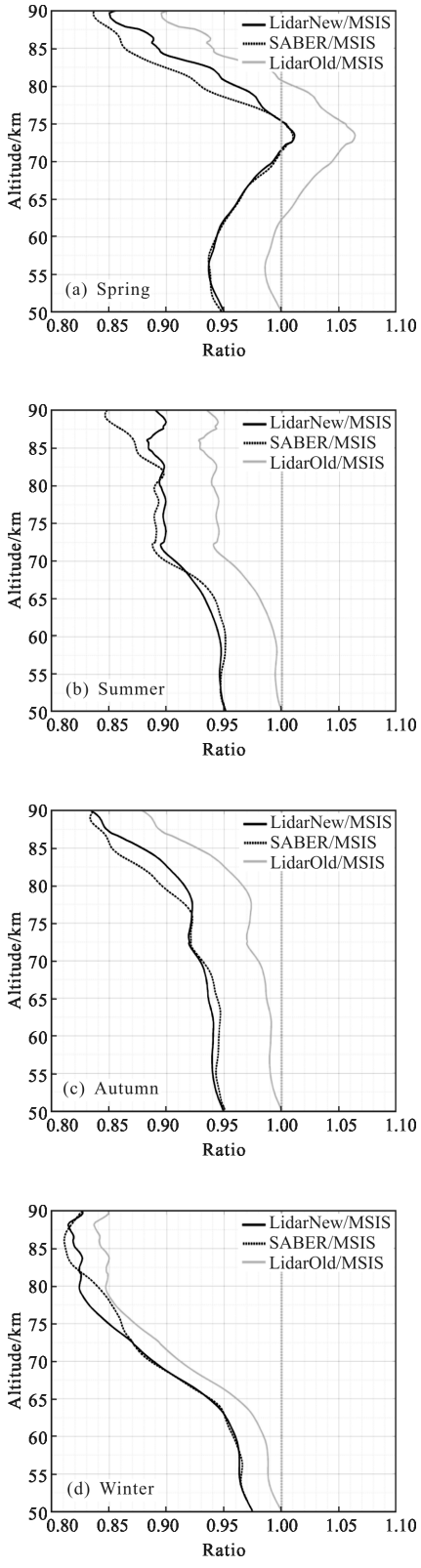

Fig.2 Mesospheric density ratio profiles in (a) spring, (b) summer, (c) autumn, (d) winter

Tab.2 Comparison of the density ratios retrieved by the new and traditional methods with satellite and model, while std_{a_b} represents the density ratio standard deviation between *a* and *b*

Season	Altitude /km	std LidarNew_ SABER	std LidarOld_ SABER	std lidarNew_ MSIS
Spring	50–75	0.18%	5.03%	4.47%
	75–90	2.49%	7.18%	8.68%
Summer	50–75	0.57%	4.68%	7.17%
	75–90	2.14%	6.23%	10.59%
Autumn	50–75	0.45%	4.66%	6.48%
	75–90	1.69%	6.36%	11.33%
Winter	50–75	0.24%	2.41%	7.78%
	75–90	1.20%	2.20%	17.40%

4 Conclusion

Our proposed algorithm for lidar density derivation has significantly improved the retrieval accuracy. Thus it is more proper to use the TIMED/SABER satellite data, instead of MSIS−00 model, as the reference density. Mesospheric densities measured by the MARMOT lidar in Golmud were consistent with the TIMED/SABER satellite results, but mostly lower that the MSIS −00 model, with the largest discrepancies occurred at 75 −90 km in winter. MARMOT lidar has provided reliable measurements of mesospheric density in the northeast part of Tibetan Plateau area, where other ground-based measurements of middle atmosphere were extremely sparse. The MSIS −00 model showed large discrepancies with observations (both lidar and satellite) in this region, thus would need further evaluation and modifications.

References:

[1] Roble R G, Dickinson R E. How will changes in carbon dioxide and methane modify the mean structure of the mesosphere and thermosphere [J]. ***Geophysical Research Letters***, 1990, 16(12): 1441−1444.

[2] Holton J R. The influence of gravity wave breaking on the general circulation of the middle atmosphere [J]. ***Journal of the Atmospheric Sciences***, 1983, 40(10): 2497-2507.

[3] Liu H L, Roble R G. A study of a self-generated stratospheric sudden warming and its mesospheric & ndash; lower thermospheric impacts using the coupled TIME-GCM/CCM3 [J]. ***Journal of Geophysical Research: Atmospheres***, 2012, 107(D23): ACL-1-ACL15-18.

[4] Yuan T, Thurairajah B, She C Y, et al. Wind and temperature response of midlatitude mesopause region to the 2009 Sudden Stratospheric Warming [J]. ***Journal of Geophysical Research Atmospheres***, 2012, 117(D9): 1-8.

[5] Wilson R, Chanin M L, Hauchecorne A. Gravity waves in the middle atmosphere observed by Rayleigh lidar: 1. Case studies [J]. ***Journal of Geophysical Research Atmospheres***, 1991, 96(D3): 5153-5167.

[6] Qian L, Solomon S C. Thermospheric density: an overview of temporal and spatial variations[J]. ***Space Science Reviews***, 2012, 168(1-4): 147-173.

[7] Pertsev N N, Semenov A I, Shefov N N. Long-term variations of temperature and neutral density of the mid-latitude middle atmosphere by rocket and optical data [C]// 17th ESA Symposium on European Rocket and Balloon Programmes and Related Research, 2005.

[8] Champion K S W. Middle atmosphere density data and comparison with models [J]. ***Advances in Space Research***, 1990, 10(6): 17-26.

[9] Rapp M, Gumbel J, Lübken F J. Absolute density measurements in the middle atmosphere [J]. ***Annales Geophysicae***, 2001, 19(5): 571-580.

[10] Hauchecorne A, Chanin M L. Density and temperature profiles obtained by Lidar between 35 km and 70 km [J]. ***Geophysical Research Letters***, 1980, 7(8): 565-568..

[11] Shibata T, Kobuchi M, Maeda M. Measurements of density and temperature profiles in the middle atmosphere with a XeF lidar[J]. ***Applied Optics***, 1986, 25(5): 685-688.

[12] McKenzie R L. Method of atmospheric density measurements during shuttle entry using ultraviolet-laser Rayleigh scattering [J]. ***Journal of Spacecraft***, 1988, 26(1): 56-64.

[13] Deng P, Zhang T, Wei C, et al. Lidar measurement for atmospheric density and temperature in middle atmosphere over Hefei [J]. ***Infrared and Laser Engineering***, 2017, 46 (7): 0730003. (in Chinese)

[14] Qiao S, Pan W, Zhu K, et al. Initial Results of lidar measured middle atmosphere temperatures over Tibetan Plateau [J]. ***Atmospheric and Oceanic Science Letters***, 2014, 7(3): 213-217.

[15] Yu T, Pan W, Zhu K Y, et al. Preliminary analysis of mesospheric summer temperature measurements in Golmud [J]. ***Infrared and laser Engineering***, 2016, 45(12): 1211005.

[16] Remsberg E E, Marshall B T, Garcia-Comas M, et al. Assessment of the quality of the Version 1.07 temperature-versus-pressure profiles of the middle atmosphere from TIMED/SABER [J]. ***Journal of Geophysical Research Atmospheres***, 2008, 113(D17): 1641-1653.

[17] Picone J M, Hedin A E, Drob D P, et al. NRLMSISE-00 empirical model of the atmosphere: Statistical comparisons and scientific issues [J]. ***Journal of Geophysical Research Space Physics***, 2002, 107(A12): SIA-1-SIA15-16.

[18] Chu X, Gardner C S, Franke S J. Nocturnal thermal structure of the mesosphere and lower thermosphere region at Maui, Hawaii (20.7 °N), and starfire optical range, new mexico (35 °N)[J]. ***Journal of Geophysical Research Atmospheres***, 2005, 110(D9): 1-13.